

# Effects of Channel Estimation Error in the Presence of CFO on OFDM BER in Frequency-Selective Rayleigh Fading Channels

Chi-Hsiao Yih

Department of Electrical Engineering, Tamkang University, Tamsui, Taiwan

Email: chyih@ee.tku.edu.tw

**Abstract**—In this paper, we study the effects of channel estimation error on the bit-error-rate (BER) of orthogonal frequency division multiplexing (OFDM) systems in frequency-selective slowly Rayleigh fading channels. Due to the additive white Gaussian noise (AWGN) and the intercarrier interference (ICI) caused by the residual carrier frequency offset (CFO), the channel estimation based on the training symbols is not perfect. We characterize the performance degradation resulting from imperfect channel state information (CSI) by deriving the BER formulas for BPSK, QPSK, 16-QAM, and 64-QAM modulation schemes. The derived BER formulas contain no numerical integrals and can be evaluated easily and accurately. Simulation results validate the correctness of our theoretical analysis.

**Index Terms**—Orthogonal frequency division multiplexing, channel estimation, carrier frequency offset, frequency-selective Rayleigh fading, bit-error-rate, performance analysis

## I. INTRODUCTION

Orthogonal frequency division multiplexing (OFDM) has become a popular transmission technique for high-data-rate wireless communications in recent years. By dividing the whole bandwidth into subchannels and transmitting data symbols in parallel, the effective data period is enlarged and the intersymbol interference (ISI) caused by the frequency-selective fading channel can be greatly reduced [1].

When coherent modulation is employed at the transmitter, channel state information (CSI) is necessary for the demodulation of transmitted signals at the receiver. Various CSI estimators and their corresponding performance analyses have been studied and appeared in the literature. For example, the effects of channel estimation error on the system bit-error-rate (BER) performance for transparent tone in band (TTIB) modulation and pilot-symbol-assisted modulation (PSAM) without or with diversity have been analyzed in [2], [3] and [4], respectively.

The issues of channel estimation in OFDM systems have been considered in [5] where the minimum mean-square error (MMSE) and least-square (LS) channel estimators exploit the property of cyclic prefix to obtain

channel estimates. The MMSE channel estimator fully using the time and frequency domain correlations of the response of time-varying dispersive fading channels has been derived and analyzed in [6]. The authors also proposed a robust channel estimator which is insensitive to the mismatch of channel statistics.

The uses of PSAM in both time and frequency domains for time-varying frequency-selective channels have been investigated in [7]- [11] where the channel estimates of OFDM data symbols are interpolated from the neighboring two-dimensional pilot tones. To improve the spectral efficiency, a novel channel estimation scheme called coded decision directed demodulation (CD3) [12] where the pilot tones are transmitted only at the beginning of a frame and the channel estimator exploits the error correcting capability of a forward error correction decoder to reconstruct the transmitted data sequences and mitigate the effects of channel estimator error. To further alleviate the power and bandwidth overhead of pilot tones, several blind and semi-blind channel estimation algorithms have been developed for OFDM systems [13]- [17].

When the OFDM-based wireless system operates in a slowly fading multiple-access environment, the use of training (preamble) symbols to facilitate the channel estimation task has been specified in the IEEE 802.11a/g standard. [18]. The performance of channel estimator based on the long preambles in OFDM-based wireless local area networks (WLAN) was examined in [19], [20]. In [19], the authors considered the channel estimate is not only corrupted by additive white Gaussian noise (AWGN) but also by the intercarrier interference (ICI) due to the residual carrier frequency offset (CFO). In the BER analysis, it was assumed the channel estimate and the channel estimation error are uncorrelated when the interference power is small. As indicated in [21], the method presented in [19] may overestimate the BER in some situations. Instead of BER, [20] considered the mean square error (MSE) of the channel estimator as the performance index and revealed the channel estimation MSE increases at the rate of approximately the square of CFO. Some recent works [22] [23] considered OFDM channel estimation problem in the presence of CFO and phase noise. Those papers focus on the development of new channel estimation algorithms and the corresponding

This paper is based on "Effects of Channel Estimation Error on the BER Performance of OFDM Systems in Multipath Rayleigh Fading Channels," by C.-H. Yih, which appeared in the Proceedings of the 66th IEEE Vehicular Technology Conference (VTC 2007-Fall), Baltimore, USA, October, 2007. © 2008 IEEE.

BER analyses are missing.

In this paper, we consider the same scenario as in [19] and we are interested in the BER which is a more important performance metric than the channel estimation MSE. We perform the exact BER analysis for BPSK, QPSK, 16-QAM, and 64-QAM modulated OFDM signals in frequency-selective Rayleigh fading channels without any assumption on the correlation between the channel estimate and the channel estimation error. Therefore, our method and result are accurate even for large CFO and channel estimation error. Moreover, the expression of the derived BER formula is in a simple form and no numerical integration is needed to evaluate it.

The remainder of this paper is organized as follows. In Section II, we describe the system and channel model. Section III presents the BER analysis for BPSK, QPSK, 16-QAM, and 64-QAM modulated OFDM signals with imperfect CSI. Numerical results which validate the theoretical analysis are given in Section IV. Finally, Section V concludes the paper.

## II. SYSTEM MODEL

In this paper, we assume the frequency-selective Rayleigh fading channel is fixed during one transmitted frame and the channel estimation is facilitated by the preamble (training) symbols embedded in the beginning of the data frame. In mathematical form, the  $m$ th transmitted baseband OFDM symbol in a frame can be expressed as

$$x_n(m) = \frac{1}{\sqrt{N}} \sum_{k=0}^{N-1} X_k(m) e^{j2\pi nk/N}, \quad (1)$$

$$n = 0, 1, \dots, N-1; \quad m = 1, 2, \dots, M$$

where  $k$  is the index of subcarrier,  $N$  is the total number of subcarriers,  $X_k(m) \in \mathcal{X}$  are the transmitted modulation symbols, and  $M$  is the number of OFDM symbols in one frame. Four types of modulation formats  $\mathcal{X}$  are considered, namely, BPSK, QPSK, 16-QAM, and 64-QAM [24]. The first  $P$  OFDM symbols in a frame are training symbols. For each OFDM training symbol, the modulation is restricted to be BPSK and the transmitted modulation symbols at each subcarrier, denoted by  $X_k^p \in \{-\sqrt{E_b}, \sqrt{E_b}\}$  where the superscript  $p$  indicates the transmitted symbol is a "preamble", are the same for the OFDM symbol index  $m$  from 1 to  $P$ . The training symbol patterns  $X_k^p$  for  $k = 0, 1, \dots, N-1$  are known at both the transmitter and the receiver ends.

We assume the cyclic prefix of length  $N_G$  samples is inserted at the beginning of each OFDM symbol and is removed in the demodulation process [1]. Furthermore, we assume the length of cyclic prefix is longer than the maximum delay spread of the multipath fading channel and the ISI can be completely eliminated.

The transmitted OFDM signal passes through a multipath fading channel whose impulse response is represented by the tapped-delay line model [24]

$$h(t) = \sum_{l=0}^{L-1} h_l \delta(t - lT/N), \quad (2)$$

where  $L < N_G$  is the number of multipaths, the path gains  $h_l$  are independently circularly symmetric complex Gaussian random variables with mean 0 and variance  $\sigma_l^2$ ,  $\delta(\cdot)$  is the Dirac-delta function, and  $T$  is the effective OFDM symbol period. For brevity, we simply use the notation  $h_l \sim \mathcal{CN}(0, \sigma_l^2)$ .

The corresponding frequency response at subcarrier  $i$  is

$$H_i = \int_{-\infty}^{\infty} h(t) e^{-j2\pi it/T} dt = \sum_{l=0}^{L-1} h_l e^{-j2\pi il/N}. \quad (3)$$

The channel frequency response  $H_i$  is also a complex Gaussian random variable with mean 0 and variance  $\sum_{l=0}^{L-1} \sigma_l^2$ . Without loss of generality, we assume the sum of the average power of each multipath is normalized to 1, i.e.  $\sum_{l=0}^{L-1} \sigma_l^2 = 1$ .

At the beginning of a frame, the initial CFO estimate may not be accurate due to the presence of noise and the limited resource dedicated to the CFO estimation. For example, the short preambles in the WLAN system can be used to obtain the coarse CFO estimate whose accuracy can be improved by succeeding fine CFO estimation based on the long preambles [25]. The normalized CFO affecting the training symbols for channel estimation is denoted by  $\epsilon = f_\Delta T$  where  $f_\Delta$  is the CFO in Hertz. Then the  $m$ th received training symbol after performing the fast Fourier transform (FFT) is [26]

$$Y_i(m) = e^{j\theta(m)} [\alpha H_i X_i^p + I_i] + W_i(m), \quad i = 0, \dots, N-1 \quad (4)$$

where the block-dependent phase-shift term  $\theta(m) = \frac{2\pi[m(N+N_G)+N_G]\epsilon}{N} + \frac{\pi\epsilon(N-1)}{N}$ , the symbol  $\alpha = \frac{\sin \pi\epsilon}{N \sin(\pi\epsilon/N)}$ ,  $I_i = \sum_{k=0, k \neq i}^{N-1} H_k X_k^p \frac{\sin(\pi\epsilon) e^{-j\pi(k-i)/N}}{N \sin[\pi(k-i+\epsilon)/N]}$ , and  $W_i(m)$  are independently, identically, distributed (I.I.D.) from  $\mathcal{CN}(0, N_0)$ .

It is commonly assumed that the block-dependent phase-shift term  $\theta(m)$  can be perfectly compensated at the receiver by using the preambles or continual pilot tones [21,27,28] so that the decision region of the modulation symbol is independent of the OFDM symbol index  $m$ . Although this assumption is a little bit ideal, it can greatly simplify the BER analysis. The design of phase-locked loop and the effect of phase tracking error on the OFDM BER is beyond the scope of this paper.

The channel estimate of  $H_i$  based on the received training signals  $Y_i(1), Y_i(2), \dots, Y_i(P)$  is given by

$$\hat{H}_i = \frac{1}{P} \sum_{m=1}^P \frac{Y_i(m) e^{-j\theta(m)}}{X_i^p} = \alpha H_i + \hat{I}_i + \hat{W}_i, \quad i = 0, 1, \dots, N-1, \quad (5)$$

where  $\hat{I}_i = \frac{I_i}{X_i^p}$ ,  $\hat{W}_i = \frac{1}{P} \sum_{m=1}^P \frac{W_i(m) e^{-j\theta(m)}}{X_i^p} \sim \mathcal{CN}(0, \frac{N_0}{P E_b})$ . The training symbols can be utilized not only for channel estimation, but also for fine CFO estimation [29]. Therefore, it is reasonably assumed the residual CFO after the training period is quite small [30]. In practical communication systems, the phase rotation caused by

the residual CFO can be estimated and compensated by the continual pilot signal embedded in some subcarriers.

Ignoring the residual CFO after the training period, the received OFDM data symbol after the FFT is

$$Y_i(m) = H_i X_i^d(m) + W_i(m),$$

$$m = P + 1, P + 2, \dots, M; \quad i = 0, 1, \dots, N - 1 \quad (6)$$

where the superscript d indicates the transmitted modulation symbols are data symbols rather than preambles.

### III. BER ANALYSIS

There are many approaches to analyzing the BER of digital modulation schemes over fading channels [4], [24], [31]. In this paper, we consider the method described in the appendix B of [24]. First, we need the following lemma to characterize the effects of channel estimation error on the BER of various modulation schemes in OFDM systems.

*Lemma 1* [24]: Let  $X$  and  $Y$  be zero mean, correlated complex-valued Gaussian random variables and  $D_1 = \Re[XY^*]$ ,  $D_2 = \Im[XY^*]$  where  $*$  stands for the complex conjugation,  $\Re(x)$  and  $\Im(x)$  are the real part and the imaginary part of  $x$ , respectively. Then

$$P(D_1 < 0) = \frac{1}{2} \left[ 1 - \frac{\Re[\mu_{XY}]}{\sqrt{\mu_{XX}\mu_{YY} - (\Im[\mu_{XY}])^2}} \right], \quad (7)$$

$$P(D_2 < 0) = \frac{1}{2} \left[ 1 - \frac{\Im[\mu_{XY}]}{\sqrt{\mu_{XX}\mu_{YY} - (\Re[\mu_{XY}])^2}} \right], \quad (8)$$

where  $\mu_{XY} = \mathbb{E}[XY^*]$ ,  $\mu_{XX} = \mathbb{E}[XX^*]$ ,  $\mu_{YY} = \mathbb{E}[YY^*]$ , and  $\mathbb{E}[\cdot]$  denotes the probabilistic expectation.

For notational simplicity, we omit the index of OFDM data symbol  $m$  in the following discussion.

#### A. BPSK

For BPSK modulation, the FFT outputs of the OFDM data symbol are

$$Y_i = H_i X_i^d + W_i, \quad i = 0, 1, \dots, N - 1 \quad (9)$$

where  $X_i^d \in \{-\sqrt{E_b}, \sqrt{E_b}\}$  is the BPSK symbol transmitted on the  $i$ th subcarrier and we assume  $P(X_i^d = \sqrt{E_b}) = P(X_i^d = -\sqrt{E_b}) = 1/2$ . For the  $i$ th subcarrier, the decision statistics for the BPSK modulated OFDM signal with imperfect CSI is  $\Re[Y_i \hat{H}_i^*]$  and the corresponding BER is

$$P_b(i) = P\left(\Re[Y_i \hat{H}_i^*] < 0 | X_i^d = \sqrt{E_b}\right), \quad (10)$$

where  $\hat{H}_i$  is given in (5). Conditioned on the transmitted symbol  $X_i^d$ , the received signal  $Y_i$  and channel estimate  $\hat{H}_i$  are both zero mean complex Gaussian random variables. To apply Lemma 1 to obtain  $P_b(i)$ , we first compute  $\mu_{Y_i \hat{H}_i | X_i^d}$ ,  $\mu_{Y_i Y_i | X_i^d}$ , and  $\mu_{\hat{H}_i \hat{H}_i | X_i^d}$  as follows.

$$\begin{aligned} \mu_{Y_i \hat{H}_i | X_i^d} &= \mathbb{E}[Y_i \hat{H}_i^* | X_i^d] \\ &= \mathbb{E}[(H_i X_i^d + W_i)(\alpha H_i^* + \hat{I}_i^* + \hat{W}_i^*) | X_i^d] \\ &= \alpha X_i^d + \mathbb{E}[H_i \hat{I}_i^* | X_i^d]. \end{aligned} \quad (11)$$

Since  $\hat{I}_i = \sum_{k=0, k \neq i}^{N-1} H_k \frac{X_k^p}{X_i^p} \frac{\sin(\pi\epsilon) e^{-j\pi(k-i)/N}}{N \sin[\pi(k-i+\epsilon)/N]}$ , the expectation  $\mathbb{E}[H_i \hat{I}_i^*]$  in (11) can be computed as

$$\begin{aligned} \mathbb{E}[H_i \hat{I}_i^*] &= \sum_{k=0, k \neq i}^{N-1} \mathbb{E}[H_i H_k^*] \frac{X_k^p}{X_i^p} \frac{\sin(\pi\epsilon) e^{j\pi(k-i)/N}}{N \sin[\pi(k-i+\epsilon)/N]}. \end{aligned} \quad (12)$$

To evaluate (12), we must compute  $\mathbb{E}[H_i H_k^*]$  for  $i \neq k$  first. Since  $H_i = \sum_{l=0}^{L-1} h_l e^{-j2\pi i l / N}$ , the expectation  $\mathbb{E}[H_i H_k^*]$  is given by

$$\begin{aligned} \rho_{i,k} &= \mathbb{E}[H_i H_k^*] \\ &= \begin{cases} 1, & i = k \\ \sum_{l=0}^{L-1} \sigma_l^2 e^{j2\pi(k-i)l/N}, & i \neq k \end{cases}. \end{aligned} \quad (13)$$

Next, we compute  $\mu_{Y_i Y_i | X_i^d}$  as

$$\begin{aligned} \mu_{Y_i Y_i | X_i^d} &= \mathbb{E}[Y_i Y_i^* | X_i^d] \\ &= |X_i^d|^2 + N_0. \end{aligned} \quad (14)$$

Finally, the  $\mu_{\hat{H}_i \hat{H}_i | X_i^d}$  is given by

$$\begin{aligned} \mu_{\hat{H}_i \hat{H}_i | X_i^d} &= \mathbb{E}[\hat{H}_i \hat{H}_i^* | X_i^d] \\ &= \mathbb{E}\left[\left(\alpha H_i + \hat{I}_i + \hat{W}_i\right)\left(\alpha H_i^* + \hat{I}_i^* + \hat{W}_i^*\right)\right] \\ &= \alpha^2 + \frac{\mathbb{E}[|I_i|^2]}{|X_i^p|^2} + \frac{N_0}{PE_b} + 2\Re(\alpha \mathbb{E}[H_i \hat{I}_i^*]). \end{aligned} \quad (15)$$

The expectation  $\mathbb{E}[|I_i|^2]$  in (15) is

$$\begin{aligned} \mathbb{E}[|I_i|^2] &= \sum_{k_1=0, k_1 \neq i}^{N-1} \sum_{k_2=0, k_2 \neq i}^{N-1} \frac{\rho_{k_1, k_2} X_{k_1}^p X_{k_2}^p \sin^2(\pi\epsilon) e^{-j\pi(k_1-k_2)/N}}{N^2 \phi(k_1, i) \phi(k_2, i)} \end{aligned} \quad (16)$$

where  $\phi(k, i) = \sin[\pi(k-i+\epsilon)/N]$ .

For subcarrier  $i$ , the BER of the BPSK modulated OFDM signal with imperfect channel estimate can be evaluated by Lemma 1 as

$$\begin{aligned} P_b^{\text{BPSK}}(i) &= P\left(\Re[Y_i \hat{H}_i^*] < 0 | X_i^d = \sqrt{E_b}\right) \\ &= \frac{1}{2} \left( 1 - \frac{\Re[\mu_{Y_i \hat{H}_i | X_i^d}]}{\sqrt{\mu_{Y_i Y_i | X_i^d} \mu_{\hat{H}_i \hat{H}_i | X_i^d} - (\Im[\mu_{Y_i \hat{H}_i | X_i^d}])^2}} \right), \end{aligned} \quad (17)$$

where  $\mu_{Y_i \hat{H}_i | X_i^d}$ ,  $\mu_{Y_i Y_i | X_i^d}$  and  $\mu_{\hat{H}_i \hat{H}_i | X_i^d}$  are given in (11), (14), and (15) with  $X_i^d = \sqrt{E_b}$ . Finally, the average BER over all subcarriers is

$$P_b^{\text{BPSK}} = \frac{1}{N} \sum_{i=0}^{N-1} P_b^{\text{BPSK}}(i). \quad (18)$$

From the expression in (17), we know the subcarrier BER  $P_b^{\text{BPSK}}(i)$  is not only a function of subcarrier index  $i$  but also a function of the training symbols  $X_k^p$  due to the effect of CFO. In fact, by carefully inspecting the derivation of (17), it is easily seen the dependency of  $P_b^{\text{BPSK}}(i)$  on  $X_k^p$  is through the ICI term  $I_i$  which is a direct consequence of CFO. On the other hand, if the channel estimation is performed under perfect CFO estimation (i.e.  $\epsilon = 0$ ), then  $\alpha = 1$ ,  $\mu_{Y_i \hat{H}_i | X_i^d} = X_i^d =$

$\sqrt{E_b}$ ,  $\mu_{Y_i Y_i | X_i^d} = |X_i^d|^2 + N_0 = E_b + N_0$ , and  $\mu_{\hat{H}_i \hat{H}_i | X_i^d} = 1 + \frac{N_0}{P E_b}$ . In this case, the subcarrier BER  $P_b^{\text{BPSK}}(i)$  is the same for all  $i = 0, 1, \dots, N - 1$  and the average BER  $P_b^{\text{BPSK}}$  can be simplified as

$$P_b^{\text{BPSK}} = \frac{1}{2} \left( 1 - \frac{1}{\sqrt{\left(1 + \frac{N_0}{E_b}\right) \left(1 + \frac{N_0}{P E_b}\right)}} \right). \quad (19)$$

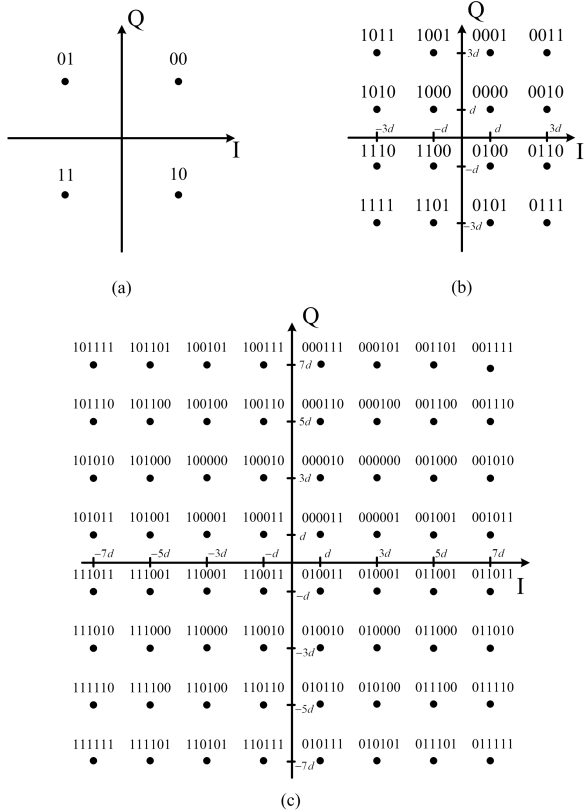


Figure 1. (a) QPSK constellation with Gray encoding. (b) 16-QAM constellation with Gray encoding. (c) 64-QAM constellation with Gray encoding.

**B. QPSK**

The constellation of QPSK is denoted by

$$\mathcal{X} = \left\{ \frac{[(2i - 1) + (2q - 1)j]\sqrt{E_s}}{\sqrt{2}}; i, q \in \{0, 1\} \right\},$$

where  $j = \sqrt{-1}$  and  $E_s$  is the symbol energy. Two information bits are mapped into a QPSK constellation symbol by the Gray encoding [24] shown in Fig. 1(a).

To generate the decision variable for the QPSK symbol  $X_i^d$  of subcarrier  $i$ , the constellation of the demodulated signal  $Y_i$  is scaled and rotated by the corresponding channel estimate  $\hat{H}_i$ . For each QPSK symbol, we only need to derive the BER of the most significant bit (MSB) since the least significant bit (LSB) has the same BER as the MSB. To compute the BER of the MSB of the QPSK constellation symbol, we consider two QPSK constellation symbols  $\frac{(1+j)\sqrt{E_s}}{\sqrt{2}}$  and  $\frac{(-1+j)\sqrt{E_s}}{\sqrt{2}}$  were sent at the transmitter end since they have different BERs

due to imperfect CSI. This is different from the perfect CSI case where usually only one constellation symbol is considered to be sent due to the symmetry of constellation and decision boundary.

From Fig. 1(a), it is obviously the decision boundary for the MSB of the QPSK symbol is the real axis and the BER of the MSB of the subcarrier  $i$  is

$$P_b^{\text{QPSK}}(i) = \frac{1}{2} \left[ P \left( \Im[Y_i \hat{H}_i^*] < 0 | X_i^d = \frac{(1+j)\sqrt{E_s}}{\sqrt{2}} \right) + P \left( \Im[Y_i \hat{H}_i^*] < 0 | X_i^d = \frac{(-1+j)\sqrt{E_s}}{\sqrt{2}} \right) \right]. \quad (20)$$

Finally, the average BER over  $N$  subcarriers is

$$P_b^{\text{QPSK}} = \frac{1}{N} \sum_{i=0}^{N-1} P_b^{\text{QPSK}}(i). \quad (21)$$

Conditioned on  $X_i^d$ , the random variables  $Y_i$  and  $\hat{H}_i$  are complex Gaussian because they are the weighted sum of complex Gaussian random variables. Therefore, we can employ Lemma 1 to compute  $P_b^{\text{QPSK}}(i)$  where  $\mu_{Y_i \hat{H}_i | X_i^d}$ ,  $\mu_{Y_i Y_i | X_i^d}$ , and  $\mu_{\hat{H}_i \hat{H}_i | X_i^d}$  are given in (11), (14), and (15) with possible  $X_i^d$  in (20).

When the CFO is perfectly compensated (i.e.  $\epsilon = 0$ ), we have  $\alpha = 1$ ,  $\mu_{Y_i \hat{H}_i | X_i^d} = X_i^d$ ,  $\mu_{Y_i Y_i | X_i^d} = |X_i^d|^2 + N_0 = E_s + N_0$ ,  $\mu_{\hat{H}_i \hat{H}_i | X_i^d} = 1 + \frac{N_0}{P E_b}$ . In this case, the subcarrier BER  $P_b^{\text{QPSK}}(i)$  is independent of the index of subcarrier  $i$  and the average BER is given by

$$P_b^{\text{QPSK}} = \frac{1}{2} \left( 1 - \frac{1}{\sqrt{\left(2 + \frac{2N_0}{E_s}\right) \left(1 + \frac{N_0}{P E_b}\right) - 1}} \right). \quad (22)$$

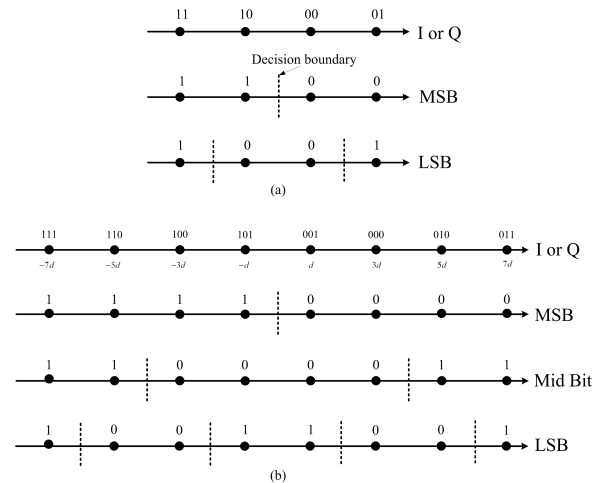


Figure 2. (a) 16-QAM bit-by-bit demapping. (b) 64-QAM bit-by-bit demapping.

**C. 16-QAM**

The 16-QAM constellation with Gray encoding is shown in Fig. 1(b). The first and third bits correspond to the inphase (I) bits, while the second and fourth bits correspond to the quadrature (Q) bits. The I and Q

components of the 16-QAM symbols are Gray encoded by assigning the bits 11, 10, 00, and 01 to the levels  $-3d$ ,  $-d$ ,  $d$ , and  $3d$  where  $d = \sqrt{E_s/10}$ .

Since we are interested in the evaluation of BER, we need to determine the decision boundary for each bit first. In Fig. 2(a), the decision boundaries for the MSB and LSB of the I/Q components are depicted [32]. Due to the symmetry of I and Q components, we only need to calculate the BER for I components.

Let  $\mathcal{X}$  be the constellation of 16-QAM where each constellation point has the same probability to be sent,  $\mathcal{X}_1$  be the set of the four 16-QAM constellation symbols having  $d$  as their I-component, i.e.  $\mathcal{X}_1 = \{x \in \mathcal{X} : \Re[x] = d\}$ . Similarly, let  $\mathcal{X}_2$  be the set of the four 16-QAM constellation symbols having  $3d$  as their I-component, i.e.  $\mathcal{X}_2 = \{x \in \mathcal{X} : \Re[x] = 3d\}$ . Since the decision boundary for the MSB bit is the imaginary axis, for subcarrier  $i$ , the BER of the MSB bit of I components is given by

$$P_b^{\text{MSB}}(i) = \frac{1}{8} \sum_{X_i^d \in \mathcal{X}_1 \cup \mathcal{X}_2} \text{P} \left\{ \Re[Y_i \hat{H}_i^*] < 0 | X_i^d \right\} \quad (23)$$

On the other hand, the decision boundaries for the LSB bit are  $I = -2d$  and  $I = 2d$  on the I-Q plane. For subcarrier  $i$ , the BER of the LSB bit of I components is

$$\begin{aligned} & P_b^{\text{LSB}}(i) \\ &= \frac{1}{8} \left\{ \sum_{X_i^d \in \mathcal{X}_1} \left[ 1 - \text{P} \left( -2d < \frac{\Re[Y_i \hat{H}_i^*]}{|\hat{H}_i|^2} < 2d | X_i^d \right) \right] \right. \\ & \left. + \sum_{X_i^d \in \mathcal{X}_2} \text{P} \left( -2d < \frac{\Re[Y_i \hat{H}_i^*]}{|\hat{H}_i|^2} < 2d | X_i^d \right) \right\}. \quad (24) \end{aligned}$$

The average BER of 16-QAM with imperfect CSI is

$$P_b^{\text{16QAM}} = \frac{1}{2N} \sum_{i=0}^{N-1} [P_b^{\text{MSB}}(i) + P_b^{\text{LSB}}(i)]. \quad (25)$$

Conditioned on the transmitted data symbol  $X_i^d$ ,  $Y_i$  and  $\hat{H}_i$  are both Gaussian. Therefore, we can use Lemma 1 to compute  $P_b^{\text{MSB}}(i)$  directly where  $\mu_{Y_i \hat{H}_i | X_i^d}$ ,  $\mu_{Y_i Y_i | X_i^d}$ , and  $\mu_{\hat{H}_i \hat{H}_i | X_i^d}$  are given in (11), (14), and (15) with  $X_i^d \in \mathcal{X}_1 \cup \mathcal{X}_2$ . However, the BER formula of  $P_b^{\text{LSB}}(i)$  is not in the exact form of Lemma 1. To apply Lemma 1 to compute  $P_b^{\text{LSB}}(i)$ , we need to transform the random variable  $Y_i$  into a new random variable  $\hat{Y}_i$  so that Lemma 1 is applicable for  $\hat{Y}_i$  and  $\hat{H}_i$ . To be more specific, we consider to compute the following probability

$$f(X_i^d, D) = \text{P} \left( \Re[Y_i \hat{H}_i^*] < |\hat{H}_i|^2 D | X_i^d \right), \quad (26)$$

where  $D$  is a real number. Let  $\hat{Y}_i = Y_i - \hat{H}_i D = H_i X_i^d + W_i - \hat{H}_i D$ , then

$$\begin{aligned} & f(X_i^d, D) = \text{P} \left( \Re[\hat{Y}_i \hat{H}_i^*] < 0 | X_i^d \right) \\ &= \frac{1}{2} \left( 1 - \frac{\Re[\mu_{\hat{Y}_i \hat{H}_i | X_i^d}]}{\sqrt{\mu_{\hat{Y}_i \hat{Y}_i | X_i^d} \mu_{\hat{H}_i \hat{H}_i | X_i^d} - (\Im[\mu_{\hat{Y}_i \hat{H}_i | X_i^d}])^2}} \right) \quad (27) \end{aligned}$$

where the second equality is a direct consequence of applying Lemma 1. Finally, we can express  $P_b^{\text{LSB}}(i)$  in terms of  $f(X_i^d, D)$  as

$$\begin{aligned} P_b^{\text{LSB}}(i) &= \frac{1}{8} \left( \sum_{X_i^d \in \mathcal{X}_1} [1 - f(X_i^d, 2d) + f(X_i^d, -2d)] \right. \\ & \left. + \sum_{X_i^d \in \mathcal{X}_2} [f(X_i^d, 2d) - f(X_i^d, -2d)] \right). \quad (28) \end{aligned}$$

To evaluate  $f(X_i^d, D)$ , we first compute

$$\mu_{\hat{Y}_i \hat{H}_i | X_i^d} = \mathbb{E}[H_i \hat{H}_i^* | X_i^d] - \mathbb{E}[\hat{H}_i \hat{H}_i^*] D, \quad (29)$$

where

$$\begin{aligned} \mathbb{E}[H_i \hat{H}_i^*] &= \mathbb{E}[H_i(\alpha H_i + \hat{I}_i + \hat{W}_i)^*] \\ &= \alpha + \mathbb{E}[H_i \hat{I}_i^*], \quad (30) \end{aligned}$$

and  $\mathbb{E}[H_i \hat{I}_i^*]$  and  $\mathbb{E}[\hat{H}_i \hat{H}_i^*]$  have been given in (12) and (15), respectively. Then we compute

$$\begin{aligned} \mu_{\hat{Y}_i \hat{Y}_i | X_i^d} &= \mathbb{E}[(Y_i - \hat{H}_i D)(Y_i - \hat{H}_i D)^* | X_i^d] \\ &= |X_i^d|^2 + N_0 + \mathbb{E}[\hat{H}_i \hat{H}_i^*] D^2 - 2\Re(\mathbb{E}[\hat{H}_i D (H_i X_i^d)^*]). \quad (31) \end{aligned}$$

When  $\epsilon = 0$ , we know  $\alpha = 1$ ,  $\hat{I}_i = 0$ , and  $\mu_{\hat{Y}_i \hat{H}_i | X_i^d}$ ,  $\mu_{\hat{Y}_i \hat{Y}_i | X_i^d}$ ,  $\mu_{\hat{H}_i \hat{H}_i | X_i^d}$  become

$$\mu_{\hat{Y}_i \hat{H}_i | X_i^d} = X_i^d - \left( 1 + \frac{N_0}{PE_b} \right) D, \quad (32)$$

$$\mu_{\hat{Y}_i \hat{Y}_i | X_i^d} = |X_i^d|^2 + N_0 + \left( 1 + \frac{N_0}{PE_b} \right) D^2 - 2D\Re[X_i^d], \quad (33)$$

and

$$\mu_{\hat{H}_i \hat{H}_i | X_i^d} = 1 + \frac{N_0}{PE_b}. \quad (34)$$

In this situation, the function  $f(X_i^d, D)$  can be simplified to (35) which is shown at the top of the next page.

#### D. 64-QAM

The 64-QAM constellation with Gray encoding is shown in Fig. 1(c). The first, third, and fifth bits correspond to the inphase bits, while the second, fourth, and sixth bits correspond to the quadrature bits. The I and Q components of the 64-QAM symbols are Gray encoded by assigning the bits 111, 110, 100, 101, 001, 000, 010, and 011 to the levels  $-7d$ ,  $-5d$ ,  $-3d$ ,  $-d$ ,  $d$ ,  $3d$ ,  $5d$ , and  $7d$  where  $d = \sqrt{E_s/42}$ . The decision boundaries for the MSB, middle bit, and LSB of the I/Q components are depicted in Fig. 2 (b) [32]. Due to the symmetry of I and Q components, we only need to calculate the BER for I components.

Let  $\mathcal{X}$  be the constellation of 64-QAM where each constellation point has the same probability to be chosen. Moreover, let  $\mathcal{X}_k$ ,  $k = 1, 2, 3, 4$  be the set of the eight 64-QAM constellation symbols having  $(2k-1)d$  as their I-component, i.e.  $\mathcal{X}_k = \{x \in \mathcal{X} : \Re[x] = (2k-1)d\}$ ,  $k = 1, 2, 3, 4$ . Since the decision boundary for the MSB bit is

$$f(X_i^d, D) = \frac{1}{2} \left( 1 - \frac{\text{Re}[X_i^d] - \left(1 + \frac{N_0}{PE_b}\right) D}{\sqrt{\left[\text{Re}[X_i^d] - \left(1 + \frac{N_0}{PE_b}\right) D\right]^2 + |X_i^d|^2 \frac{N_0}{PE_b} + N_0 \left(1 + \frac{N_0}{PE_b}\right)}} \right). \quad (35)$$

the imaginary axis, for subcarrier  $i$ , the BER of the MSB bit of I components is given by

$$P_b^{\text{MSB}}(i) = \frac{1}{32} \sum_{X_i^d \in \bigcup_{k=1}^4 \mathcal{X}_k} P\left(\Re[Y_i \hat{H}_i^*] < 0 | X_i^d\right) \quad (36)$$

On the other hand, the decision boundaries for the middle bit are  $I = -4d$  and  $I = 4d$  on the I-Q plane. For subcarrier  $i$ , the BER of the middle bit of I components  $P_b^{\text{MID}}(i)$  is given at the top of the next page. Finally, the decision boundaries for the LSB bit are  $I = -6d$ ,  $I = -2d$ ,  $I = 2d$ , and  $I = 6d$  on the I-Q plane. For subcarrier  $i$ , the BER of the LSB bit of I components  $P_b^{\text{LSB}}(i)$  is shown at the top of the next page. The average BER of 64-QAM with imperfect CSI is

$$P_b^{64\text{QAM}} = \frac{1}{3N} \sum_{i=0}^{N-1} [P_b^{\text{MSB}}(i) + P_b^{\text{MID}}(i) + P_b^{\text{LSB}}(i)]. \quad (39)$$

We can employ Lemma 1 to compute  $P_b^{\text{MSB}}(i)$  directly where  $\mu_{Y_i \hat{H}_i | X_i^d}$ ,  $\mu_{Y_i Y_i | X_i^d}$ , and  $\mu_{\hat{H}_i \hat{H}_i | X_i^d}$  are given in (11), (14), and (15) with  $X_i^d \in \bigcup_{k=1}^4 \mathcal{X}_k$ . As for  $P_b^{\text{MID}}(i)$  and  $P_b^{\text{LSB}}(i)$ , we can use the technique developed in the 16-QAM case to express  $P_b^{\text{MID}}(i)$  and  $P_b^{\text{LSB}}(i)$  in terms of  $f(X_i^d, D)$ . The results are given in (40) and (41), respectively.

#### IV. NUMERICAL RESULTS

##### A. Simulation Setup

We consider an OFDM system with  $N = 64$  subcarriers. The effective OFDM symbol period is  $T = 3.2 \mu\text{s}$  and the subcarrier frequency spacing  $f_s$  is 312.5 kHz. The received signal is sampled at the rate of 20 MHz. The power delay profile of the multipath Rayleigh fading channel is exponentially decaying and the root mean square (rms) delay spread is equal to 100 ns. We also assume the channel is fixed for the whole frame and is independent from frame to frame. These parameters and assumptions are typical for the indoor WLAN applications.

The OFDM training symbol consists of 64 subcarriers, which are modulated by the BPSK symbol of the sequence  $\mathbf{X}^p = [X_0^p \ X_1^p \ \dots \ X_{N-1}^p] = \sqrt{E_b}[\mathbf{X}_1^p \ \mathbf{X}_2^p \ \mathbf{X}_3^p \ \mathbf{X}_4^p]$ , where

$$\begin{aligned} \mathbf{X}_1^p &= [-1, -1, 1, 1, -1, 1, 1, -1, 1, 1, -1, 1, 1, -1, 1, -1, 1], \\ \mathbf{X}_2^p &= [1, 1, -1, -1, 1, -1, 1, 1, -1, 1, 1, -1, -1, 1, -1, 1], \\ \mathbf{X}_3^p &= [1, 1, 1, 1, 1, -1, -1, -1, -1, 1, -1, 1, -1, 1, 1, -1], \\ \mathbf{X}_4^p &= [-1, -1, -1, 1, 1, 1, 1, 1, -1, -1, -1, 1, -1, 1, -1, -1]. \end{aligned}$$

The training sequence  $\mathbf{X}^p$  is selected under the peak-to-average power ratio (PAPR) constraint [1], we do not try to optimize the training sequence  $\mathbf{X}^p$  at this moment.

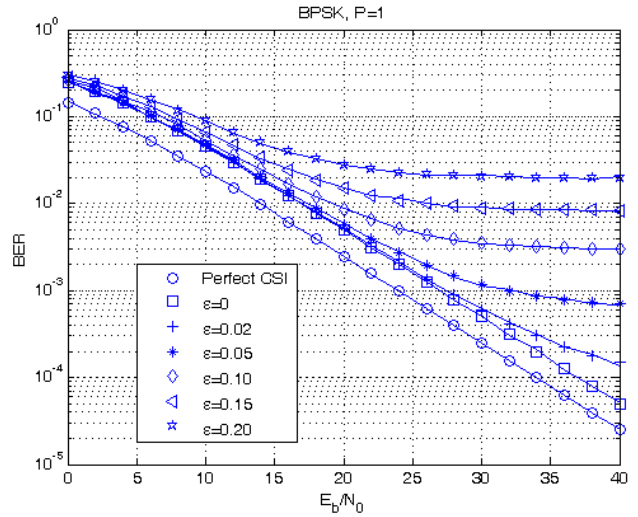


Figure 3. Effect of channel estimation error on the BER of BPSK modulated OFDM signals in multipath Rayleigh fading channels.

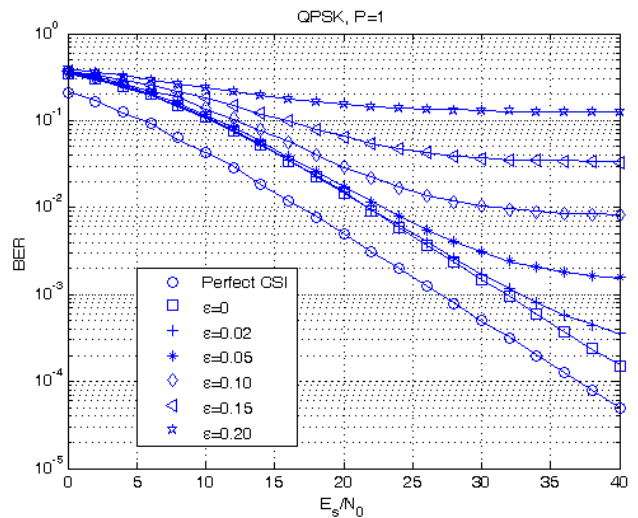


Figure 4. Effect of channel estimation error on the BER of QPSK modulated OFDM signals in multipath Rayleigh fading channels.

##### B. Results

Figs. 3, 4, 5, and 6 show the effects of channel estimation error on the BER performance of BPSK, QPSK, 16-QAM, and 64-QAM modulated OFDM signals in multipath Rayleigh fading channels, respectively. The number of training symbols  $P$  used for channel estimation is 1. The solid lines are obtained from computer simulation and the markers are computed from our theoretical results. The horizontal axis represents the modulated data symbol SNR  $E_s/N_0$ . We assume the number of the

$$P_b^{\text{MID}}(i) = \frac{1}{32} \left\{ \sum_{X_i^d \in \mathcal{X}_1 \cup \mathcal{X}_2} \left[ 1 - P \left( -4d < \frac{\Re[Y_i \hat{H}_i^*]}{|\hat{H}_i|^2} < 4d |X_i^d| \right) \right] + \sum_{X_i^d \in \mathcal{X}_3 \cup \mathcal{X}_4} P \left( -4d < \frac{\Re[Y_i \hat{H}_i^*]}{|\hat{H}_i|^2} < 4d |X_i^d| \right) \right\}. \quad (37)$$

$$P_b^{\text{LSB}}(i) = \frac{1}{32} \left\{ \sum_{X_i^d \in \mathcal{X}_1 \cup \mathcal{X}_4} \left[ P \left( -6d < \frac{\Re[Y_i \hat{H}_i^*]}{|\hat{H}_i|^2} < -2d |X_i^d| \right) + P \left( 2d < \frac{\Re[Y_i \hat{H}_i^*]}{|\hat{H}_i|^2} < 6d |X_i^d| \right) \right] + \sum_{X_i^d \in \mathcal{X}_2 \cup \mathcal{X}_3} \left[ 1 - P \left( -6d < \frac{\Re[Y_i \hat{H}_i^*]}{|\hat{H}_i|^2} < -2d |X_i^d| \right) - P \left( 2d < \frac{\Re[Y_i \hat{H}_i^*]}{|\hat{H}_i|^2} < 6d |X_i^d| \right) \right] \right\}. \quad (38)$$

$$P_b^{\text{MID}}(i) = \frac{1}{32} \left( \sum_{X_i^d \in \mathcal{X}_1 \cup \mathcal{X}_2} [1 - f(X_i^d, 4d) + f(X_i^d, -4d)] + \sum_{X_i^d \in \mathcal{X}_3 \cup \mathcal{X}_4} [f(X_i^d, 4d) - f(X_i^d, -4d)] \right), \quad (40)$$

$$P_b^{\text{LSB}}(i) = \frac{1}{32} \left( \sum_{X_i^d \in \mathcal{X}_1 \cup \mathcal{X}_4} [f(X_i^d, -2d) - f(X_i^d, -6d) + f(X_i^d, 6d) - f(X_i^d, 2d)] + \sum_{X_i^d \in \mathcal{X}_2 \cup \mathcal{X}_3} [1 - f(X_i^d, -2d) + f(X_i^d, -6d) - f(X_i^d, 6d) + f(X_i^d, 2d)] \right). \quad (41)$$

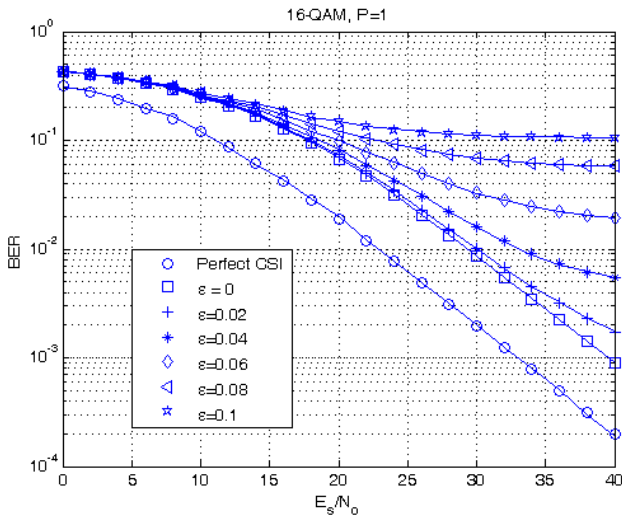


Figure 5. Effect of channel estimation error on the BER of 16-QAM modulated OFDM signals in multipath Rayleigh fading channels.

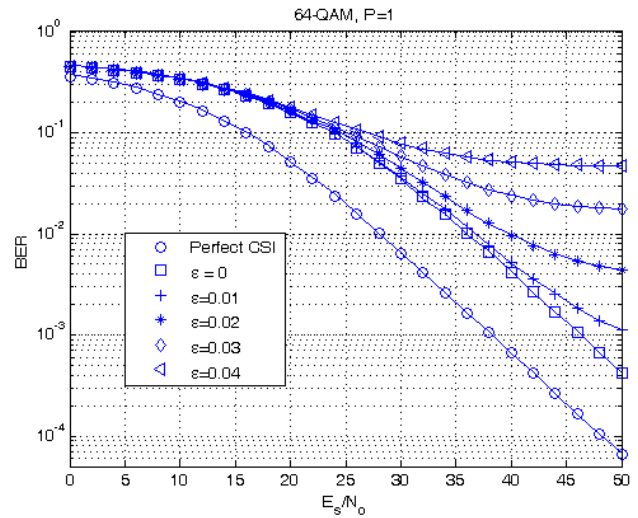


Figure 6. Effect of channel estimation error on the BER of 64-QAM modulated OFDM signals in multipath Rayleigh fading channels.

OFDM data symbols are much greater than that of the OFDM training symbols in one frame, hence the loss of power in the OFDM training symbols is negligible. Since the subcarriers of training OFDM symbols is BPSK modulated, the bit SNR  $E_b/N_0$  and symbol SNR  $E_s/N_0$  is related by  $\frac{E_b}{N_0} \log_2 |\mathcal{X}| = \frac{E_s}{N_0}$  where  $|\mathcal{X}|$  is the size of the constellation.

From Figs. 3-6, it is evident the theoretical analysis exactly matched with the simulation results for different normalized CFO  $\epsilon$ . When the CFO is perfectly com-

pensated in the channel estimation stage (i.e.  $\epsilon = 0$ ), the performance loss due to imperfect CSI is about 3 dB, 5 dB, 7 dB, and 9 dB for BPSK, QPSK, 16-QAM, and 64-QAM, respectively. As the normalized CFO  $\epsilon$  increases, the channel estimate becomes less reliable and the BER performance becomes worse. Due to the effect of ICI created by the CFO, there exist error floors when  $E_s/N_0$  is large. Finally, by examining those four figures closely, we find the performance degradation due to channel estimation error is more severe in high-order

modulation than in BPSK. That implies the high-order modulation like 64-QAM needs much more accurate CFO and channel estimation to avoid performance loss.

The influence of the number of training symbols  $P$  on the BER performance for BPSK, QPSK, 16-QAM, and 64-QAM modulated OFDM signals in Rayleigh fading channels is depicted in Fig. 7. The normalized CFO  $\epsilon$  is set to be 0.03 and all curves are drawn based on the theoretical results. When  $E_s/N_0$  is small, the BER is mainly dominated by the AWGN and the increase of  $P$  does not provide much performance gain. On the other hand, when  $E_s/N_0$  is large, the BER is mainly governed by the ICI and the increase of  $P$  does not have much performance gain. Since 16-QAM is more sensitive to channel estimation error compared to BPSK and QPSK, the larger value of  $P$  can benefit 16-QAM more than the other two types of modulation in the middle range of  $E_s/N_0$ , as can be observed in the figure.

When the residual CFO  $\epsilon$  is not zero, the dependency of BER on the training sequence  $\mathbf{X}^P$  can be identified from the expressions of  $\mu_{Y_i \hat{H}_i | X_i^p}$  and  $\mu_{\hat{H}_i \hat{H}_i | X_i^p}$ . That means the BER formulas for various modulation schemes are functions of the pilot symbols  $X_0^p, X_1^p, \dots, X_{N-1}^p$ . Since pilot symbols restricted to be BPSK, minimizing the average BER  $P_b$  over  $X_0^p, X_1^p, \dots, X_{N-1}^p$  is a combinatorial optimization problem whose computational complexity grows exponentially with the number of subcarriers  $N$ . When  $N$  is less than or equal to 16, we exhaustively search all  $2^N$  possible training sequences and find the all 1's pilot sequence  $\hat{\mathbf{X}}^P = \sqrt{E_b}[1 \ 1 \ \dots \ 1]$  and the all -1's pilot sequence  $\tilde{\mathbf{X}}^P = \sqrt{E_b}[-1 \ -1 \ \dots \ -1]$  are both the optimal training sequences in the sense of minimizing the average BER. Although  $\hat{\mathbf{X}}^P$  and  $\tilde{\mathbf{X}}^P$  achieve the minimal  $P_b$ , they both have the largest PAPR which is undesirable and problematic in OFDM systems.

When  $N = 64$ , the exhaustive search method to find the optimal training sequence  $\mathbf{X}_{\text{opt}}^P$  is impractical. To illustrate the dependency of the average BER on a specific training sequence, we consider the following three specific training sequences. The first training sequence is  $\mathbf{X}_1^P = \sqrt{E_b}[X_0^p \ X_1^p \ \dots \ X_{63}^p]$  where  $X_i^p = 1$  for  $i = 0, 1, \dots, 63$ , the second training sequence is

$$\mathbf{X}_2^P = \sqrt{E_b}[X_0^p \ X_1^p \ \dots \ X_{63}^p],$$

where

$$X_i^p = \begin{cases} -1, & i = 0, 1, \dots, 15, 48, 49, \dots, 63 \\ 1, & i = 16, 17, \dots, 47 \end{cases}$$

and the third training sequence is  $\mathbf{X}_3^P = \mathbf{X}^P$ .

Fig. 8 shows the BER curves of the BPSK and 16-QAM modulated OFDM signals with the training sequences  $\mathbf{X}_1^P, \mathbf{X}_2^P$ , and  $\mathbf{X}_3^P$ . The residual CFO  $\epsilon$  is set to be 0.03. When  $E_s/N_0$  is less than 20 dB, we find the BER curves corresponding to the BPSK and 16-QAM modulated OFDM signals with three training sequences are almost the same because the multipath fading and AWGN govern the performance in this SNR region. As  $E_s/N_0$  increases, the effect of ICI which is a function of the

training sequence becomes dominant and the performance difference among the three training sequences becomes apparent. Depending on the desired operating SNR, the selection of suitable training sequence may have great influence on the average BER of OFDM systems.

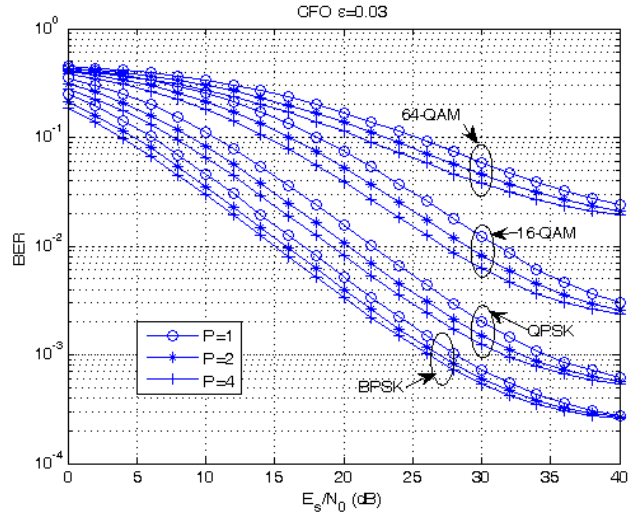


Figure 7. The BER performance of BPSK, QPSK, 16-QAM, and 64-QAM modulated OFDM signals with different numbers of training symbols.

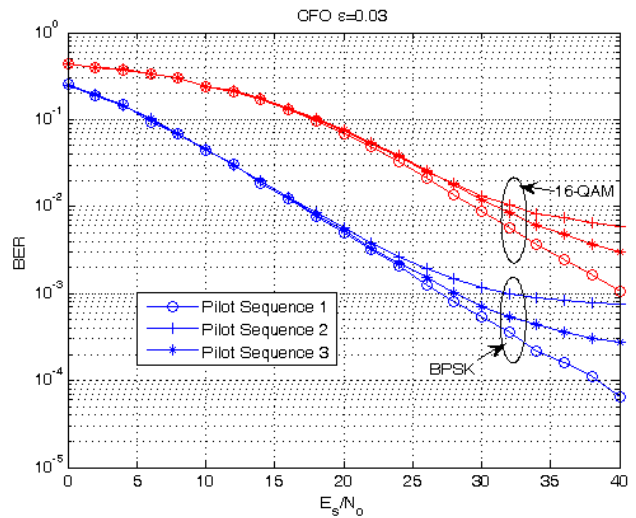


Figure 8. The BER performance of BPSK and 16-QAM modulated OFDM signal with three different training sequences.

## V. CONCLUSIONS

We investigated the effects of channel estimation error on the BER performance of OFDM systems in multipath fading channels. For BPSK, QPSK, 16-QAM, and 64-QAM modulated OFDM signals, we derived the BER formula characterizing the performance degradation due to imperfect channel estimation. Computer simulations were conducted to verify the accuracy of our theoretical analyses. The BER analysis can be extended to frequency-selective Rician fading channels by generalizing the



Lemma 1 to the case of nonzero mean complex-valued Gaussian random variables. From the BER expression, we learn the BER depends on the patterns of training sequences. The design of optimal training sequence in the sense of minimizing the average BER subject to the PAPR constraint is left for future studies.

#### REFERENCES

- [1] R. Nee and R. Prasad, *OFDM for Wireless Multimedia Communications*. Norwell, MA: Artech House, 2000.
- [2] J. K. Cavers, "The performance of phased locked transparent tone in band with symmetric phase detection," *IEEE Trans. Commun.*, vol. 39, no. 9, pp. 1389-1399, Sep. 1991.
- [3] J. K. Cavers, "An analysis of pilot-symbol-assisted modulation for Rayleigh fading channels," *IEEE Trans. Veh. Technol.*, vol. 40, no. 5, pp. 1389-1399, Nov. 1991.
- [4] L. Cao and N. C. Beaulieu, "Exact error-rate analysis of diversity 16-QAM with channel estimation error," *IEEE Trans. Commun.*, vol. 52, no. 6, pp. 1019-1028, June 2004.
- [5] J.-J. van de Beek, O. Edfors, M. Sandell, S. K. Wilson, and P. O. Börjesson, "On channel estimation in OFDM systems," in Proc. 45th IEEE Vehicular Technology Conf., Chicago, IL, July 1995, pp. 815V819.
- [6] Y. Li, L. J. Cimini, and N. R. Sollenberger, "Robust channel estimation for OFDM systems with rapid dispersive fading channels" *IEEE Trans. Commun.*, vol. 46, no. 7, pp. 902-915, Jul. 1998.
- [7] P. Hoehner, S. Kaiser and P. Robertson, "Two-dimensional pilot-symbol-aided channel estimation by Wiener filtering," *Proc. Int. Conf. Acoustics, Speech, and Signal Processing*, pp. 1845-1848, Munich, Germany, Apr. 1997.
- [8] Y. Li, "Pilot-symbol-aided channel estimation for OFDM in wireless systems," *IEEE Trans. Veh. Technol.*, vol. 49, no. 4, pp. 1207-1215, Jul. 2000.
- [9] L. Hanzo, W. Webb, and T. Keller, *Single- and Multi-carrier Quadrature Amplitude Modulation: Principles and Applications for Personal Communications, WLANs and Broadcasting*, Chichester: John Wiley & Sons, Inc. 2000.
- [10] R. Negi and J. Cioffi, "Pilot tone selection for channel estimation in a mobile OFDM system," *IEEE Trans. Consum. Electron.*, vol. 44, no. 8, pp. 1122-1128, Aug. 1998.
- [11] M. Morelli and U. Mengali, "A comparison of pilot-aided channel estimation methods for OFDM systems," *IEEE Trans. Signal Processing*, vol. 49, no. 12, pp. 3065-3073, Dec. 2001.
- [12] V. Mignone and A. Morello, "CD3-OFDM: a novel demodulation scheme for fixed and mobile receivers," *IEEE Trans. Commun.*, vol. 44, no. 5, pp. 1144-1151, Sep. 1996.
- [13] J. Heath and G. Giannakis, "Exploiting input cyclostationarity for blind channel identification in OFDM systems," *IEEE Trans. Signal Process.*, vol. 47, no. 3, pp. 848-856, Mar. 1999.
- [14] Y. Song, S. Roy, and L. Akers, "Joint blind estimation of channel and data symbols in OFDM," *Proc. IEEE Veh. Technol. Conf.*, pp. 46-50, May 2000.
- [15] S. Zhou and G. Giannakis, "Finite-alphabet based channel estimation for OFDM and related multicarrier systems," *IEEE Trans. Commun.*, vol. 49, no. 9, pp. 1402-1414, Aug. 2001.
- [16] B. Muquet, M. de Courville, and P. Duhamel, "Subspace-based blind and semi-blind channel estimation for OFDM systems," *IEEE Trans. Signal Process.*, vol. 50, no. 7, pp. 1699-1712, Jul. 2002.
- [17] L. Mazet, V. Buzenac-Settineri, M. de Courville, and P. Duhamel, "An EM based semi-blind channel estimation algorithm designed for OFDM systems," *Proc. Thirty-Sixth Asilomar Conf. on Signals, Systems and Computers*, pp. 1642-1646, Nov. 2002.
- [18] *Wireless LAN Media Access Control (MAC) and Physical Layer (PHY) Specification: High-Speed Physical Layer in the 5 GHz Band*, Piscataway, NJ: IEEE Std. 802.11a, Sep. 1999.
- [19] H. Cheon and D. Hong, "Effect of channel estimation error in OFDM-based WLAN", *IEEE Commun. Letter*, vol. 6, no. 5, pp. 190-192, May 2002.
- [20] L. Weng, E. K. S. Au, P. W. C. Chan, R. D. Murch, R. S. Cheng, W. H. Mow, and V. K. N. Lau, "Effect of carrier frequency offset on channel estimation for SISO/MIMO-OFDM systems," *IEEE Trans. Wireless Commun.*, vol. 6, no. 5, pp. 1854-1863, May 2007.
- [21] L. Rugini and P. Banelli, "BER of OFDM systems impaired by carrier frequency offset in multipath fading channels", *IEEE Trans. on Wireless Commun.*, vol. 4, pp. 2279-2288, Sep. 2005.
- [22] S. Wu and Y. Bar-Ness, "OFDM channel estimation in the presence of frequency offset and phase noise," *Proc. IEEE Int. Conf. Commun.*, pp. 3366-3370, May 2003.
- [23] D. D. Lin, R. A. Pacheco, T. J. Lim, and D. Hatzinakos, "Optimal OFDM channel estimation with carrier frequency offset and phase noise", *Proc. IEEE Wireless Commun. and Networking Conf.*, pp. 1050-1055, Las Vegas, USA, Apr. 2006.
- [24] J. G. Proakis, *Digital Communications*. New York: McGraw-Hill, 2001.
- [25] J. Heiskala and J. Terry, *OFDM Wireless WLANs: A Theoretical and Practical Guide*. Sams Publishing, 2001.
- [26] X. Ma, C. Tepedelenlioglu, G. B. Giannakis, and S. Barbarossa, "Non-data-aided carrier offset estimators for OFDM with null subcarriers: identifiability, algorithms, and performance," *IEEE J. Sel. Areas Commun.*, vol. 19, no. 12, pp. 2504-2515, Dec. 2001.
- [27] K. Sathananthan and C. Tellambura, "Probability of error calculation of OFDM systems with frequency offset," *IEEE Trans. Commun.*, vol. 49, no. 11, pp. 1884-1888, Nov. 2001.
- [28] T. Pollet, M. van Bladel, and M. Moeneclaey, "BER sensitivity of OFDM systems to carrier frequency offset and Wiener phase noise," *IEEE Trans. Commun.*, vol. 43, no. 234, pp. 191-193, Feb./Mar./Apr. 1995.
- [29] T. M. Schmidl and D. C. Cox, "Robust frequency and timing synchronization for OFDM," *IEEE Trans. Commun.*, vol. 45, no. 12, pp. 1613-1621, Dec. 1997.
- [30] J. Li, G. Liu, and G. B. Giannakis, "Carrier frequency offset estimation for OFDM-based WLANs," *IEEE Signal Proc. Letters*, vol. 8, no. 3, pp. 80-82, March 2001.
- [31] M. K. Simon and M.-S. Alouini, *Digital Communications over Fading Channels*. New Jersey: John Wiley & Sons, Inc. 2005.
- [32] X. Tang, M.-S. Alouini, and A. J. Goldsmith, "Effect of channel estimation error on M-QAM BER performance in Rayleigh fading," *IEEE Trans. Commun.*, vol. 47, no. 12, pp. 1856-1864, Dec. 1999.

**Chi-Hsiao Yih** received the B.S. degree in control engineering from the National Chiao-Tung University, Taiwan, in 1993. and the M.S. and Ph.D. degrees in electrical engineering from the University of Maryland, College Park, in 1999 and 2003, respectively.

From 2003 to 2005, he was with the Genesyslogic Inc. as a senior IC design engineer. Since August 2005, he has been with the Department of Electrical Engineering, Tamkang University, where he is currently an Assistant Professor. His research interests include digital communications, error control coding, and statistical signal processing.